Current-Driven IGBT Gate Driver Circuit Considering Four Operation Regions

Souma Yamamoto, Yudai Abe, Akio Iwabuchi, Jun-ichi Matsuda, Anna Kuwana, Haoyang Du, Takafumi Kamio, Takashi Hosono, Shogo Katayama, and Haruo Kobayashi

Abstract IGBTs have both features of MOSFETs and Bipolar Junction Transistors (BJTs) and are used in a wide range of fields as power semiconductor devices. However, for their usage, there are problems of parasitic capacitances among their terminals, switching loss due to tail current at turnoff, and excessive overshoot owing to parasitic inductances of wirings. In this paper, first, we introduce the current-driven IGBT gate driver circuit with improving the trade-off between the output voltage excess overshoot and switching loss by dividing the operation region into

S. Yamamoto (✉) · Y. Abe · J. Matsuda · A. Kuwana · H. Du · T. Kamio · T. Hosono · S. Katayama · H. Kobayashi
Division of Electronics and Informatics, Faculty of Science and Technology, Gunma University, 1-5-1 Tenjin-cho, Kiryu-shi, Gunma 376-8515, Japan
e-mail: t160d126@gunma-u.ac.jp

Y. Abe
e-mail: t191d003@gunma-u.ac.jp

J. Matsuda
e-mail: jun-ichi.matsuda@nifty.com

A. Kuwana
e-mail: kuwana.anna@gunma-u.ac.jp

H. Du
e-mail: t201d606@gunma-u.ac.jp

T. Kamio
e-mail: t170d037@gunma-u.ac.jp

T. Hosono
e-mail: t201d072@gunma-u.ac.jp

S. Katayama
e-mail: t15304906@gunma-u.ac.jp

H. Kobayashi
e-mail: koba@gunma-u.ac.jp

A. Iwabuchi
Sanken Electric Co., Ltd, 3-6-3 Kitano, Niiza-shi, Saitama 352-0003, Japan
e-mail: aiwabuch@ms2.sanken-ele.co.jp

X.-S. Yang et al. (eds.), *Proceedings of Seventh International Congress on Information and Communication Technology*, Lecture Notes in Networks and Systems 465,
https://doi.org/10.1007/978-981-19-2397-5_33

four parts with the current drive during IGBT turnoff and pulling a proper gate current depending on the region. Compared with the voltage drive, the overshoot at IGBT turnoff is improved to −32% and the switching loss to −35%. Next, we show a devised circuit that detects changes in the gate voltage of a current-driven IGBT gate driver circuit to respond to changes in the voltage and current on the collector side of the IGBT; this enables real-time automatic discrimination of the IGBT operation region. This automatic discrimination of the operation region demonstrates the feasibility of the automatic current control.

Keywords Insulated gate bipolar transistor · Gate driver · Current driven · Switching loss · Overshoot · Operation regions · Automatic control · Differentiating circuit

1 Introduction

Insulated Gate Bipolar Transistors (IGBTs) have the features of MOSFETs and Bipolar Junction Transistors (BJTs) as power semiconductor devices and are used in a wide range of fields from automotive applications for Electric Vehicle (EV) motor control to industrial equipment and household appliances. In order to utilize power electronics in the Internet of Things (IoT) systems, superior performances of IGBTs and their driver circuits are of great importance [1, 2].

For usage of IGBTs, there are some problems such as parasitic capacitances among their terminals, switching loss due to tail current at turnoff [2], and excessive overshoot owing to parasitic inductances of wirings [3]. The large gate capacitances make the realization of the IGBT driver circuit a challenging and differentiating technology.

In this paper, first, we introduce our previously proposed current-driven IGBT gate driver to achieve an appropriate trade-off between the output voltage overshoot and the switching loss at IGBT turnoff. We show that it can be improved by dividing the IGBT turnoff current drive into four driving regions. Compared with the voltage driver, the overshoot and switching loss at IGBT turnoff are improved to −32% and −35%, respectively [4, 5].

Next, we show an automatic detection circuit for the IGBT operation region to cope with changes in the voltage and current on the collector side of the IGBT. The possibility of the automatic current control is demonstrated by the automatic discrimination of the operation region. In the voltage driver, it is necessary to change the drive resistance during switching, which makes the control more complicated. However, the current drive can simplify the driver circuit control design [6].

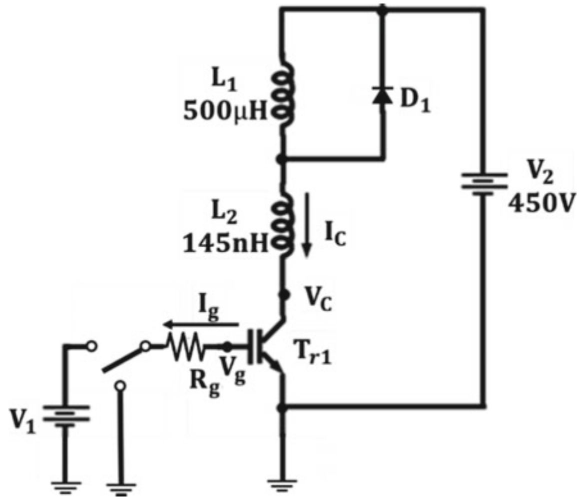

Fig. 1 Voltage-driven IGBT turnoff characterization circuit

2 IGBT Turnoff Characteristics

2.1 Evaluation Circuit Using Voltage Driver

Figure 1 shows an evaluation circuit for IGBT turnoff characteristics using a voltage driver. The input voltage V_1 drives the gate voltage of T_{r1} (IGBT). When the switch is connected to V_1 side, the collector current I_c flows gradually owing to V_1. When T_{r1} turns on, the current flows through the path of $L_1 \Rightarrow L_2 \Rightarrow T_{r1} \Rightarrow V_2 \Rightarrow L_1$. When T_{r1} turns off, the current flows through the path of$L_1 \Rightarrow D_1 \Rightarrow L_1$. The supply voltage V_2 is the bias voltage at turnoff and L_2 models the parasitic inductance of the lead wire, while R_g is the gate resistance, V_g is the gate voltage, and I_g is the gate current. Figure 2 shows the turnoff characteristics, and we see that when V_g decreases, the IGBT turns off and I_c becomes zero, and there we observe the overshoot voltage at the collector (V_c).

2.2 Relationship Between Overshoot and Switching Loss

Figure 3 shows the simulated result of the relationship between overshoot and switching loss in case that the value of the gate resistance (R_g) in the circuit diagram of Fig. 1 is changed from 30 to 300 Ω. It is observed from Fig. 3 that there is a compromise between overshoot and switching loss. In Sect. 3, we will compare the trade-offs in the voltage drive and current drive cases.

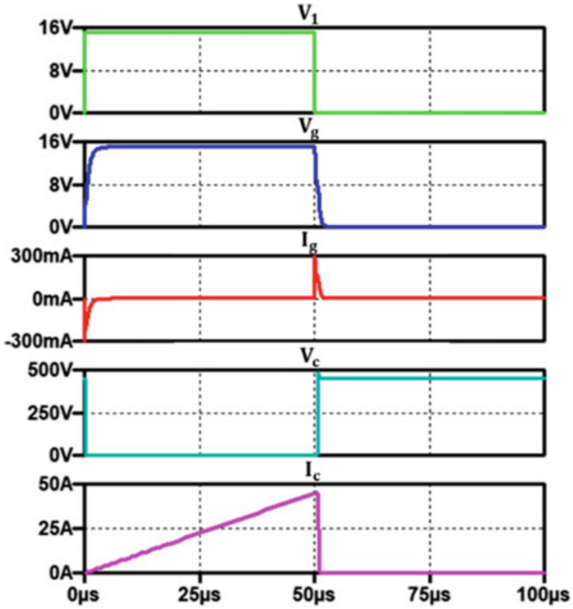

Fig. 2 Waveforms in the voltage-driven IGBT circuit during turnoff

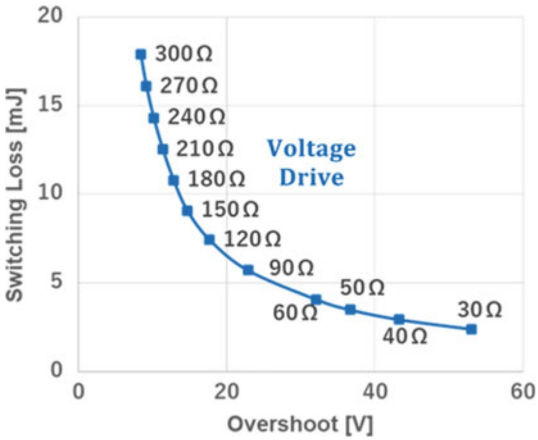

Fig. 3 Simulation result of the output voltage overshoot and the switching loss in Fig. 1

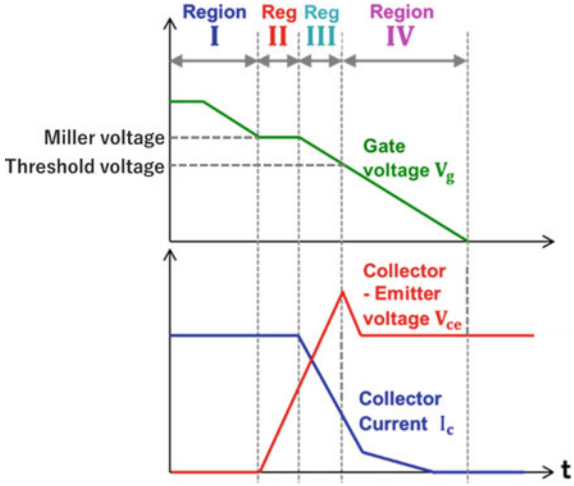

Fig. 4 Four operation regions during turnoff

3 Current-Driven IGBT Gate Driver Circuit

3.1 Gate Driver Control Current

In this section, the current driver is investigated to control the collector voltage by varying the gate current in four operation regions at turnoff, based on the gate voltage [5]. Figure 4 shows the four operation regions at turnoff. In Region I (Fig. 4), the gate voltage decreases from the saturation voltage to the Miller voltage; there is no effect on overshoot and switching loss. On the contrary, in Region II, the gate voltage is almost constant; this is the Miller effect owing to the parasitic Miller capacitance between the collector and the gate of the IGBT. In this region, there is a trade-off between the switching loss and the slew rate; the switching loss can be suppressed by adjusting the slew rate. In Region III, the gate voltage decreases from the Miller voltage to the threshold voltage. In this region, there is a trade-off relationship between overshoot and switching loss, and we found that it can be improved by controlling the overshoot to an appropriate value. In Region IV, the gate voltage goes from the IGBT threshold voltage to zero, and there is no effect on overshoot and switching loss.

3.2 Current Driver Circuit

The current-driven IGBT driver circuit for simulation is shown in Fig. 5, and the simulated waveforms of the currents I_1–I_6 are shown in Fig. 6. As shown in Fig. 5, this driver circuit controls the gate voltage by pulling out the current I_6 from the IGBT gate; I_6 is the sum of the currents I_2 to I_5 which are switched by the control.

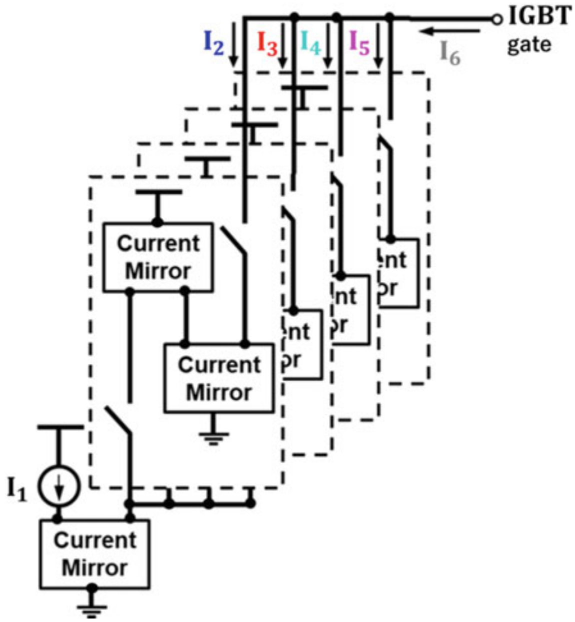

Fig. 5 Current-driven IGBT driver circuit

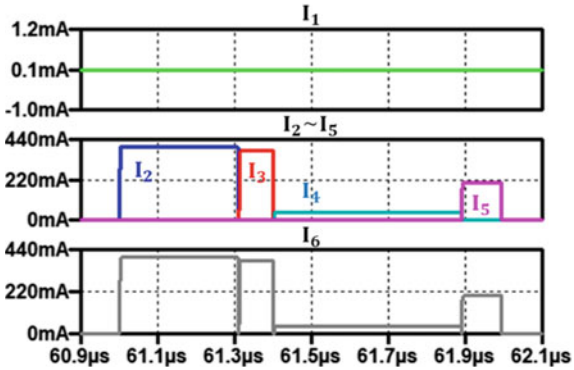

Fig. 6 Control current waveforms of the current-driven driver

This driver circuit is used to evaluate the turnoff characteristics of IGBTs. The current drive evaluation circuit is shown in Fig. 7, and its turnoff characteristics are shown in Fig. 8; the pulling gate current I_g is varied depending on the operation region of the gate voltage V_g. In Region IV, the MOSFET in the output stage of the current mirror circuit goes from saturation region to linear region, so it is difficult to control the gate current I_g. A comparison of the relationship between overshoot and switching loss for the voltage drive in Fig. 1 and the current drive in Fig. 7 is shown in Fig. 9. We see that the overshoot and switching loss of the current drive can be improved to −32% and −35%, respectively, compared to the voltage drive. The power loss on the gate side is mainly due to the energy-charged and discharged in the parasitic

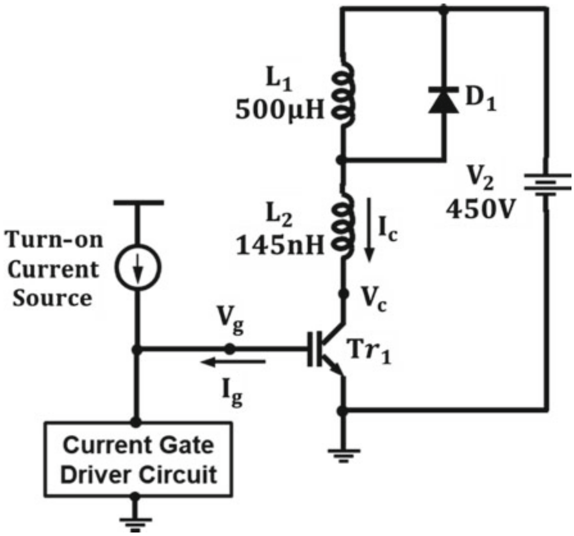

Fig. 7 Current-driven IGBT turnoff characterization circuit

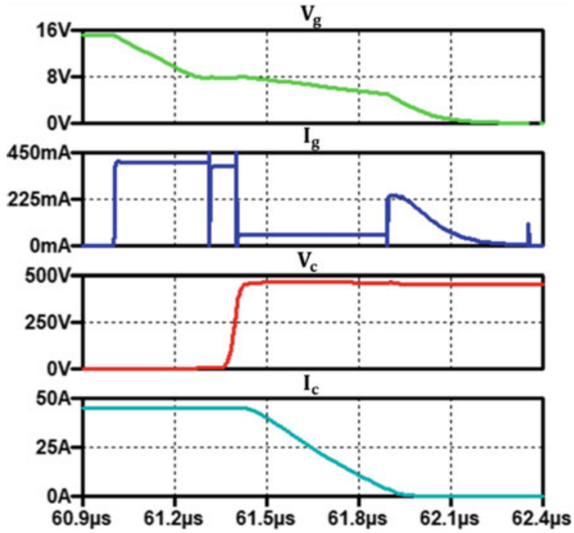

Fig. 8 Waveforms in the current-driven IGBT circuit during turnoff

capacitance, resulting in a loss of several microjoules, whereas on the collector side, the loss is several millijoules; so only the loss on the collector side is considered in this paper.

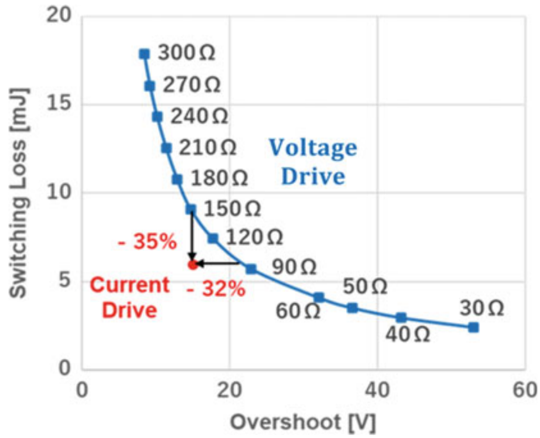

Fig. 9 Overshoots and switching losses of the voltage driver and current driver IGBT circuits

3.3 *Automatic Discrimination of Operation Regions (Analog Value)*

Next, we consider the automatic discrimination of the operation regions of the current-driven IGBT gate driver. As shown in Fig. 10, the operation region is automatically determined by observing the value of the IGBT gate voltage using a differentiation circuit. First, Fig. 11a shows the ideal waveform of the output voltage ($-V_o$) of the differentiation circuit for the waveform of the gate voltage V_g. As shown in this waveform, the steeper the slope of V_g is, the larger the ideal value of $-V_o$ becomes. However, the observed waveform of $-V_o$ is shown in Fig. 11b. Figure 12 shows an enlarged view of Fig. 11b, where a glitch of up to 35 mV appears at the boundary of each operation region. The glitch of up to 35 mV appears at the boundary of each

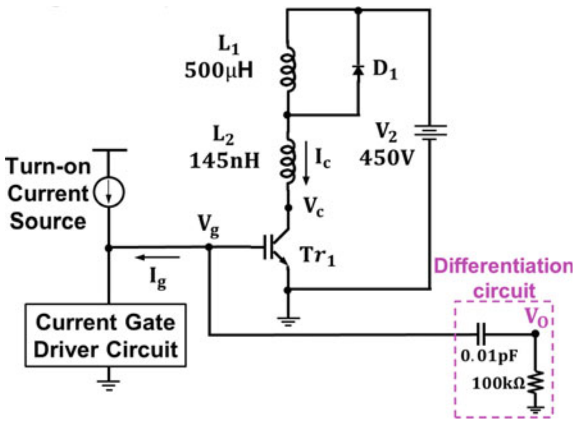

Fig. 10 Differentiation circuit for determining operation region

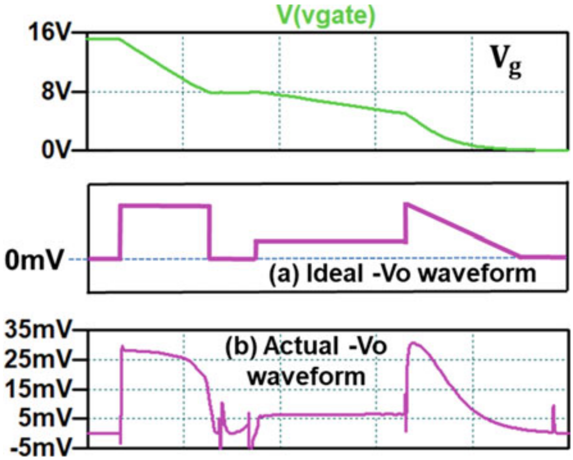

Fig. 11 Output voltage $-V_o$ waveforms of the differentiation circuit

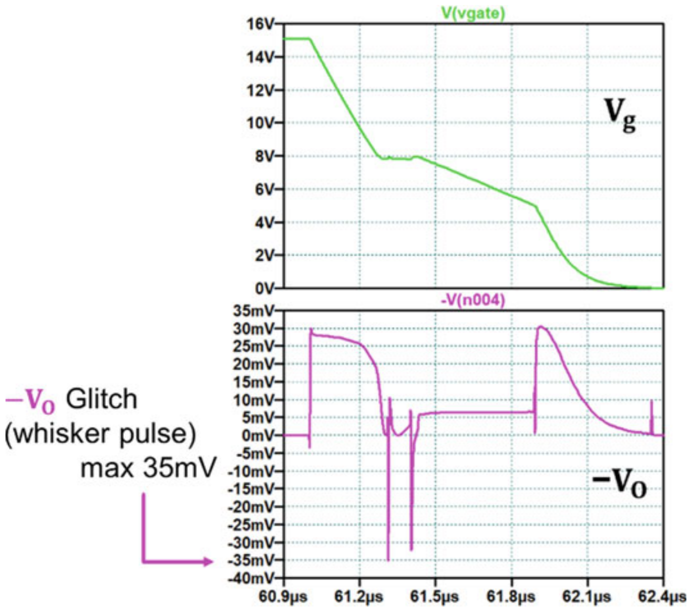

Fig. 12 Enlarged of actual $-V_o$ waveform

operation region, so it may be difficult to discriminate the operation region accurately near the operation region boundary.

Now we consider that as shown in Fig. 13, the output ($-V_o$) of the differentiation circuit is passed through an RC low-pass filter, and the output ($-V_{o2}$) of the filter is used as the final output for glitch reduction. The simulation results are shown in

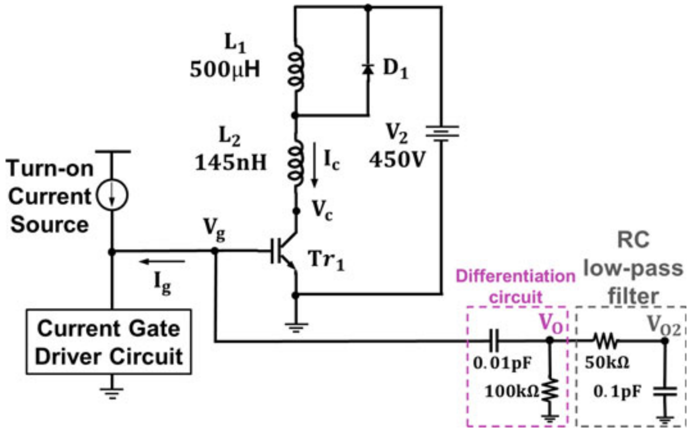

Fig. 13 Addition of an RC low-pass filter

Fig. 14, where the glitch is reduced to a maximum of 6 mV at the final output ($-V_{o2}$) by adding the RC low-pass filter. However, since there are still glitches, we also consider the operation region discrimination using an active differentiator with an

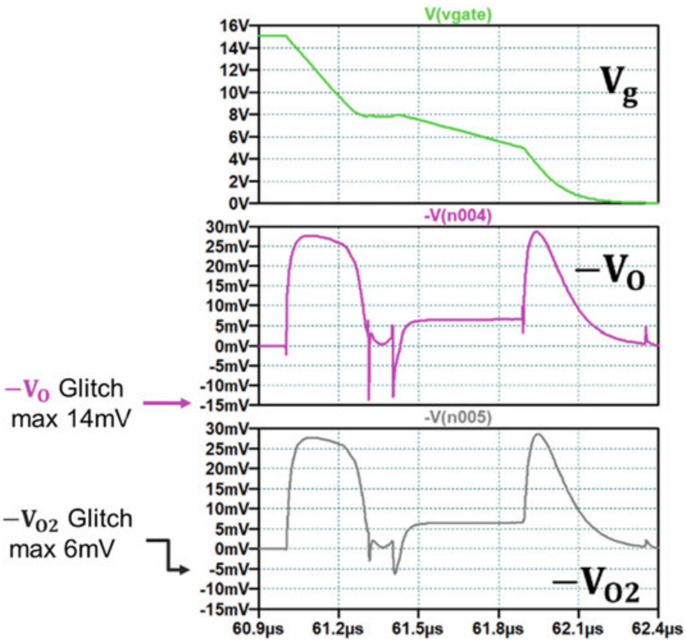

Fig. 14 Output voltage $-V_{o2}$ waveform of the RC low-pass filter

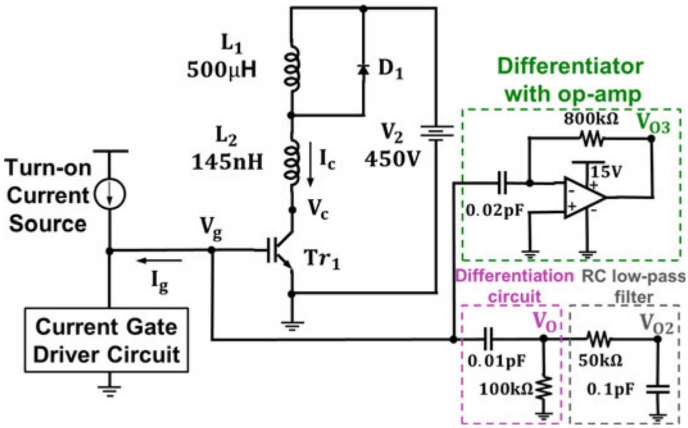

Fig. 15 Addition of an active differentiator with an operational amplifier

operational amplifier. Notice that the operational amplifier has a limited bandwidth, and it is a low-pass characteristic itself.

As shown in Fig. 15, the operation region is automatically determined by observing the value of the IGBT gate voltage using a differentiator with an operational amplifier. Its model is UniversalOpamp2, which is a general-purpose operational amplifier model provided by LTspice. The simulation results of Fig. 15 are shown in Fig. 16. The output of the differentiator with an operational amplifier is V_{o3}. The glitch was reduced to nearly zero when compared to $-V_{o2}$. On the contrary, there is a disadvantage that the time between the change in the slope of V_g and the change in the value of V_{o3} (the time between the change in the operation region and the detection of V_{o3}) is delayed compared to the time between the change in the operation region and the detection of $-V_{o2}$.

3.4 Automatic Discrimination of Operation Regions (Digital Value)

Next, we consider using the detected value of V_{o3} to represent the operation region as a digital value. Since V_{o3} is an analog value, it is unclear at which point the boundary of the operation region is determined. Therefore, the boundary between the operation regions should be clarified by converting V_{o3} into four digital values. Figure 17 shows the operation region discrimination circuit using comparators and Set-Reset Flip-Flops (SRFFs). Initially, all SRFFs are reset by the reset signal so that their outputs $Q = 0$. The detected V_{o3} value is input to the comparators and converted into four digital values (RSo1 to RSo4) as shown in Fig. 18a. This enables real-time discrimination of the operation regions. Table 1 shows the conversion table of the digital values of the outputs RSo1 to RSo4 and the operation regions.

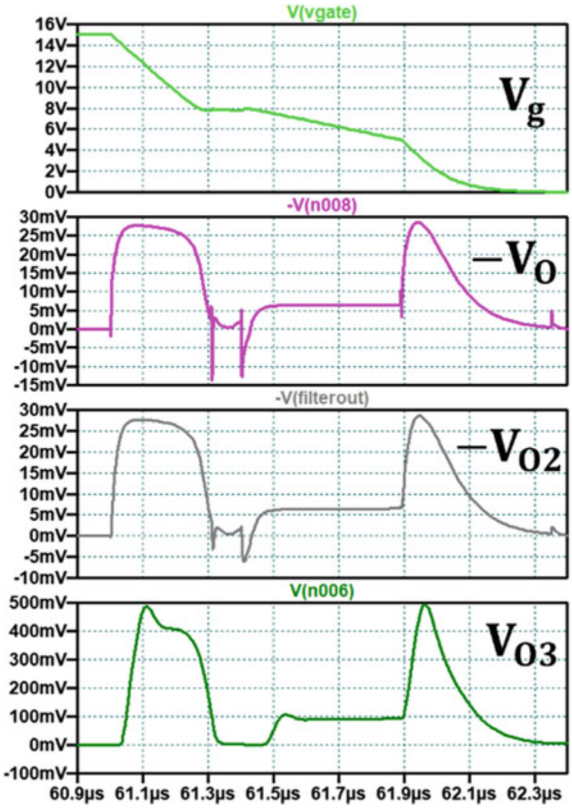

Fig. 16 Output voltage V_{o3} waveform of differentiator with an operational amplifier

A remaining issue for the design completion is as follows. As shown in Fig. 18b, the boundary of the actual operation regions is the point where the slope of V_g changes. On the contrary, in the detected operation regions shown in Fig. 18c, the rising point of each RSo1–RSo4 is considered as the boundary of the operation region. We see by comparing (b) and (c) that the detected operation region is later than the actual operation region.

Figure 19 shows the improved operation region discrimination circuit, where two comparators and two SRFFs (SRFFX, SRFFY) are added for the reduction of the detection delay of the boundary between Region I and Region II. The detected V_{o3} value is input to the comparators and converted into four digital values (RSo1–RSo4) as shown in Fig. 20a. We see that the detection delay at the boundary between Region I and Region II in Fig. 18c is reduced as shown in Fig. 20c.

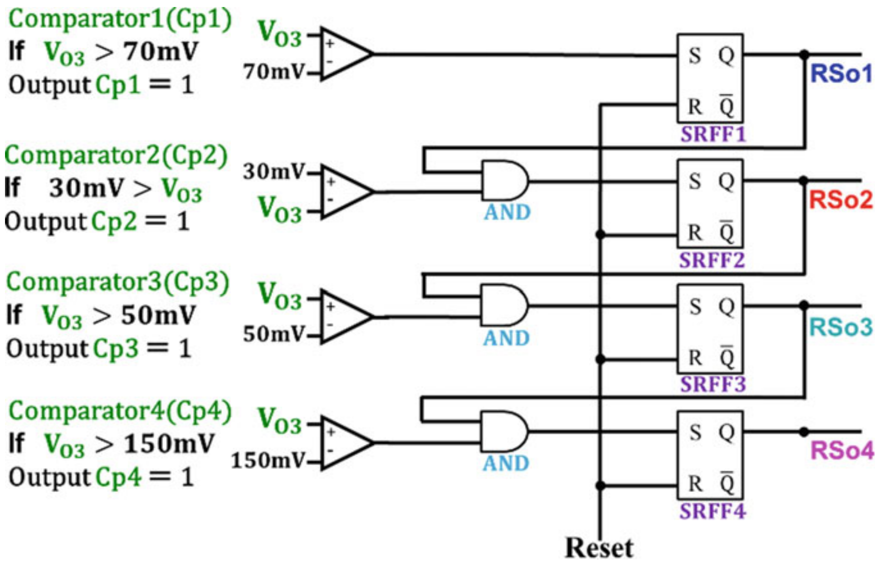

Fig. 17 Discrimination circuit of operation region by comparators and SRFFs

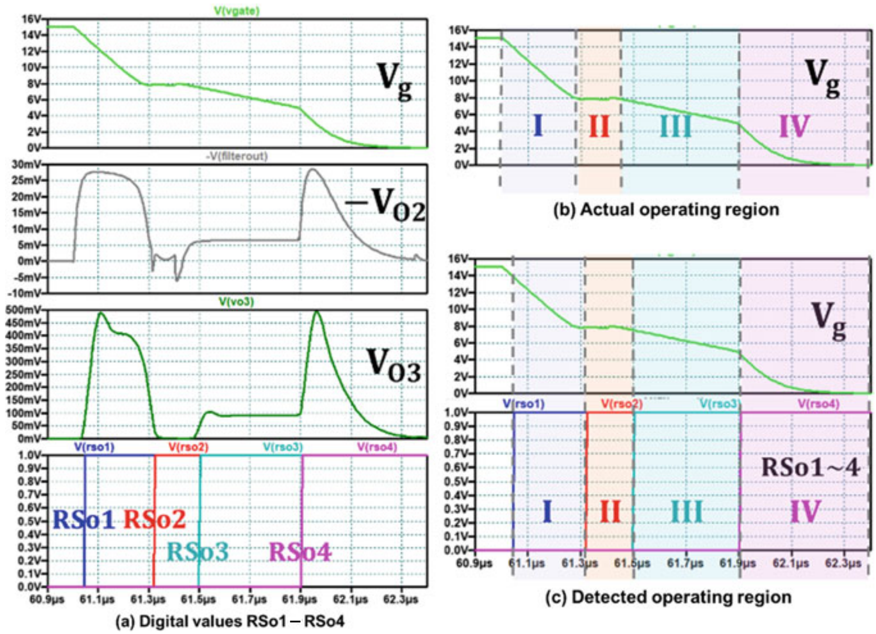

Fig. 18 RSo1–RSo4 waveforms for the circuit in Fig. 17

Table 1 Conversion table between digital values and operation regions

	RSo1	RSo2	RSo3	RSo4
Region I	1	0	0	0
Region II	1	1	0	0
Region III	1	1	1	0
Region IV	1	1	1	1

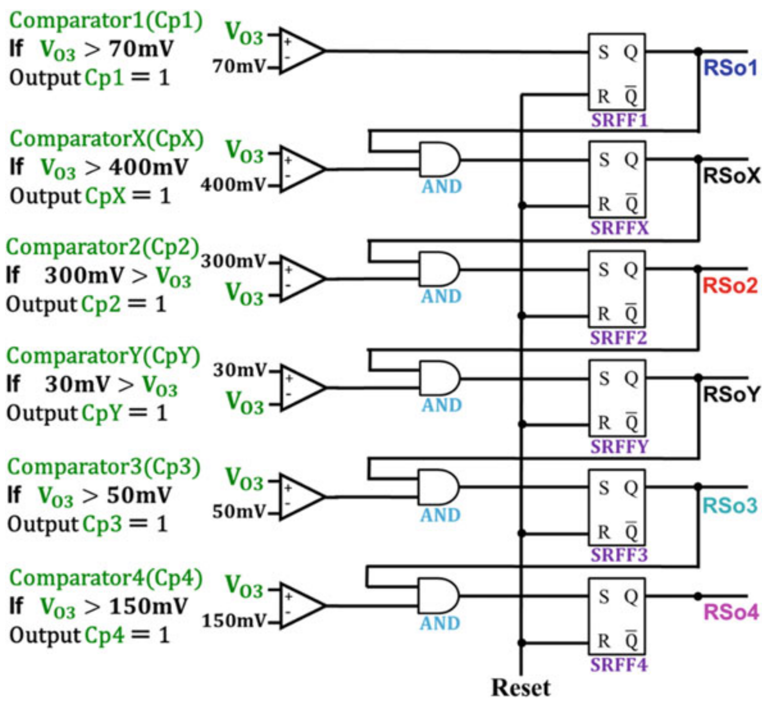

Fig. 19 Improved discrimination circuit of operation region by comparators and SRFFs

4 Conclusion

This paper has described the current-driven IGBT gate driver circuit which draws different currents depending on four operation regions. It was shown that compared with the voltage-driven circuit, the output voltage excess overshoot at IGBT turnoff was improved to −32%, and the switching loss was improved to −35%. We have devised a circuit to detect the change in gate voltage of the current-driven IGBT gate driver, which enables automatic discrimination of the IGBT operation region.

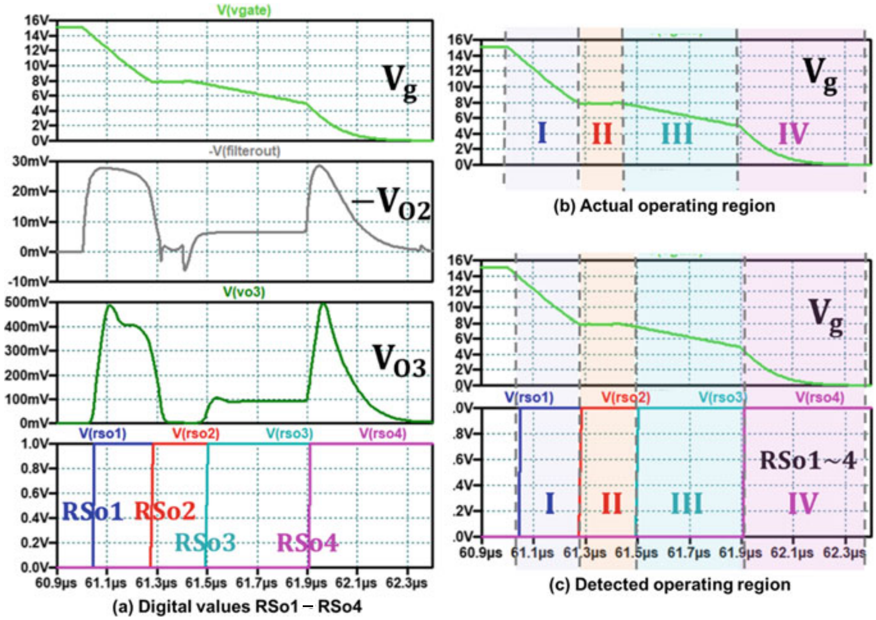

Fig. 20 RSo1–RSo4 waveforms for the circuit in Fig. 19

References

1. Takamiya M (2021) Digitalized power electronics for incorporating IoT and AI. In: 2021 international conference on solid state devices and materials, pp 712–713, Virtual
2. Takamiya M, Miyazaki K, Obara H, Sai T, Wada K, Sakurai T (2017) Power electronics 2.0: IoT-connected and AI-controlled power electronics operating optimally for each user. In: 2017 29th international symposium on power semiconductor devices and IC's. IEEE, Sapporo, pp 29–32. https://doi.org/10.23919/ISPSD.2017.7988875
3. Katada R, Hata K, Yamauchi Y, Wang T, Morikawa R, Wu C, Sai T, Chen P, Takamiya M (2021) Digital gate driving (DGD) is double-edged sword: how to avoid huge voltage overshoots caused by DGD for GaN FETs. In: 2021 IEEE energy conversion congress & exposition, pp 5412–5416, Virtual. https://doi.org/10.1109/ECCE47101.2021.9595264
4. Abe Y, Iwabuchi A, Matsuda J, Kuwana A, Ida T, Shibasaki Y, Kobayashi H (2020) Low power loss IGBT driver circuit using current drive. In: 2020 International SoC design conference. IEEE, Yeosu, pp 135–136. https://doi.org/10.1109/ISOCC50952.2020.9333104
5. Abe Y, Iwabuchi A, Matsuda J, Yamamoto S, Kuwana A, Du H, Kamio T, Hosono T, Kobayashi H (2021) Study on current-driven IGBT driver circuit. In: 36th international technical conference on circuits/systems, computers and communications. IEEE, Jeju, pp 1–4. https://doi.org/10.1109/ITC-CSCC52171.2021.9501438
6. Tokita Y, Abe S, Tsukuda M, Omura I (2019) On the effect of constant current source in active gate drive. In: Kyushu Section joint conference of electronics, electrical and information processing engineering. Fukuoka, p 620